JPET Fast Forward. Published on February 4, 2004 as DOI:10.1124/jpet.103.063370

Mouse "reduced in osteosclerosis" transporter (Roct) functions as an organic anion transporter 3 (mOAT3) and is localized at abluminal membrane of blood-brain barrier

Sumio Ohtsuki, Tazuru Kikkawa, Shinobu Mori, Satoko Hori, Hitomi Takanaga, Masaki Otagiri, Tetsuya Terasaki

Department of Molecular Biopharmacy and Genetics, Graduate School of Pharmaceutical Sciences (S.O., T.K., S.M., S.H., H.T. and T.T.), and New Industry Creation Hatchery Center (S.O., S.H., H.T. and T.T.), Tohoku University, Aoba, Aramaki, Aoba-ku, Sendai 980-8578, Japan.

SORST of Japan Science and Technology Agency (JST), Japan (S.O., S.H., H.T. and T.T.).

Faculty of Pharmaceutical Sciences, Kumamoto University, 5-1 Oe-honmachi, Kumamoto 862-0973, Japan (M.O.)

a) Running title: Mouse Roct functions as OAT3 and is localized at the BBB

b) Author for correspondence: Professor Tetsuya Terasaki,

Department of Molecular Biopharmacy and Genetics, Graduate School of Pharmaceutical Sciences, Tohoku University, Aoba, Aramaki, Aoba-ku, Sendai 980-8578, Japan

Voice: +81-22-217-6831 FAX: +81-22-217-6886

E-mail: terasaki@mail.pharm.tohoku.ac.jp

c) The number of text pages: 39

Number of tables: 3

Number of figures: 6

Number of references: 30

Number of words in the Abstract: 214

Number of words in the Introduction: 434

Number of words in the Discussion: 1496

d) Abbreviations: BBB, blood-brain barrier; CSF, cerebrospinal fluid; DMSO,

JPET Fast Forward. Published on February 4, 2004 as DOI: 10.1124/jpet.103.063370
This article has not been copyedited and formatted. The final version may differ from this version.

dimethyl sulfoxide; E_1S, estrone sulfate; GFAP, glial fibrillary acidic protein; GSH, glutathione reduced form; GSSG, glutathione oxidized form; OAT, organic anion transporter; oatp2, organic anion transporting polypeptide 2; OCT, organic cation transporter; PAH, *p*-aminohippuric acid; PCR, polymerase chain reaction; Roct, reduced in osteosclerosis transporter; V-ATPase, vacuolar proton ATPase.

e) Recommended section: Absorption, Distribution, Metabolism and Excretion

Abstract

The “reduced in osteosclerosis” transporter (Roct), which shows decreased expression in the osteosclerosis (*oc*) mutant mouse, has high homology with rat and human organic anion transporter 3 (OAT3). However, its transport properties and involvement in bone turnover are poorly understood. Here, we examined Roct-mediated transport using a *Xenopus laevis* oocyte expression system. Roct-expressing oocytes exhibited uptake of [^{3}H]estrone sulfate, [^{3}H]*p*-aminohippuric acid, [^{3}H]benzylpenicillin, [^{3}H]estradiol 17β-glucronide, [^{3}H]indoxyl sulfate, [^{14}C]indomethacin, [^{3}H]homovanillic acid, [^{3}H]cimetidine, [^{14}C]glutarate, [^{14}C]salicylic acid and [^{3}H]methotrexate. Furthermore, the uptakes of [^{3}H]benzylpenicillin by Roct co-expressed with Na^{+}-dicarboxylate cotransporter were trans-stimulated by glutarate preloading, and [^{3}H]estrone sulfate uptake showed a similar tendency, suggesting that Roct is a dicarboxylate exchanger. [^{3}H]Benzylpenicillin uptake by Roct was inhibited by OAT3 substrates and inhibitors, and by sulfate or glucuronide conjugates, and compounds involved in bone turnover. Roct mRNA is expressed abundantly in the kidney, and was also detected in the brain, choroid plexus and eye. Immunohistochemical analysis revealed that Roct is localized in brain capillary

endothelial cells. These results indicate that the transport properties and tissue distribution of Roct are similar to those of OAT3, suggesting that Roct functions as mouse OAT3. Since Roct is expressed in the kidney and at the blood-brain barrier, it may play a role in the excretion of substrates such as conjugates and bone turnover factors.

Human autosomal recessive osteopetrosis is a severe disease characterized by an increase of bone density. The murine mutation osteosclerosis (oc) has a similar phenotype to the human disease, and the reduced in osteosclerosis transporter (Roct) and osteoclast-specific vacuolar proton ATPase (V-ATPase) subunit genes were identified as being located in the *oc* locus and related to the *oc* phenotype (Brady et al., 1999; Scimeca et al., 2000).

Expression of Roct protein is reduced in the kidney of mice homozygous for *oc* mutation (Brady et al., 1999), although the involvement of Roct in osteopetrosis is still unknown. V-ATPase is involved in the formation of an acidic extracellular compartment for solubilization of bone minerals by osteoclasts, and its 1.6-kb 5' sequence, including the first ATG, is deleted in the *oc* mutant mouse (Scimeca et al., 2000). The loss of V-ATPase function is thought to be a direct cause of osteopetrosis in the *oc* mutant. Nevertheless, chronic renal failure leads to bone disease, including osteosclerosis (Adams, 2002), and recessive osteopetrosis in humans is associated with neural defects (Sobacchi et al., 2001). These symptoms may not be directly associated with bone overgrowth owing to the defect of V-ATPase function.

Roct cDNA encodes 537 amino acids, and its predicted amino acid

sequence contains 12 putative transmembrane domains and shows high homology with those of organic anion transporters (OATs), especially rat OAT3 (rOAT3; 92.4%) and human OAT3 (hOAT3, SLC22A8; 78.0%). OAT3 is expressed in renal microtubules and at the blood-brain barrier (BBB), and is considered to play an important role in the excretion of uremic toxins and neurotransmitter metabolites (Cha et al., 2001; Deguchi et al., 2002; Ohtsuki et al., 2002; Mori et al., 2003). Furthermore, in humans, OAT3 and V-ATPase genes are located in the same genomic locus (ch11q11-13), like Roct and V-ATPase in mouse (Heaney et al., 1998; Cha et al., 2001). Therefore, if Roct functions as an OAT3 in the mouse kidney and BBB, impairment of its function would explain the relationship between osteopetrosis, renal failure and neural defects. Indeed, Roct has been suggested to function at the kidney and choroid plexus based on a study of Roct knock-out mice (Sweet et al., 2002). As regards function, Roct cRNA-injected oocytes exhibited uptake of *p*-aminohippuric acid (PAH), estrone sulfate (E_1S) and taurocholate (Sweet et al., 2002), but otherwise, the transport properties and expression of Roct are still unclear.

The purposes of the present work were firstly, to clarify the transport properties of Roct using the *Xenopus laevis* oocyte expression system and,

secondly, to investigate the expression and localization of Roct by means of Northern blot, RT-PCR and immunohistochemical studies.

JPET Fast Forward. Published on February 4, 2004 as DOI: 10.1124/jpet.103.063370
This article has not been copyedited and formatted. The final version may differ from this version.

MATERIALS AND METHODS

Animals

Adult male C57BL6 mice, weighing 23 to 27 g, were purchased from Nippon SLC (Hamamatsu, Japan). Mature female *Xenopus laevis* were purchased from Hamamatsu Kyozai (Hamamatsu, Japan) and maintained in a controlled environment as described by Goldin (1992). All experiments were approved by the Animal Care Committee, Graduate School of Pharmaceutical Sciences, Tohoku University.

Reagents

The pGEM-HEN vector was a kind gift from Dr. T. Abe (Tohoku University, Japan). *para*-[glycyl-2-^{3}H]Aminohippuric acid ([^{3}H]PAH, 3.25 Ci/mmol), [estradiol-6, 7-^{3}H (N)]estradiol 17β-D-glucuronide ([^{3}H]estradiol 17β-D-glucuronide, 45.0 Ci/mmol), [6, 7-^{3}H (N)]estrone sulfate ammonium salt ([^{3}H]E_1S, 43.1 Ci/mmol) and [^{3}H(G)]digoxin ([^{3}H]digoxin, 19.0 Ci/mmol) were purchased from NEN Life Science Products (Boston, MA). [*phenyl*-4(n)-^{3}H]Benzylpenicillin ([^{3}H]benzylpenicilin, 20.0 Ci/mmol) and [*N-methyl*-^{3}H]cimetidine ([^{3}H]cimetidine, 14.8 Ci/mmol) were purchased from

Amersham Biosciences (Piscataway, NJ). [7-^{14}C]Salicylic acid ([^{14}C]salicylic acid, 55.5 mCi/mmol) and [2-^{14}C]indomethacin ([^{14}C]indomethacin, 20.0 mCi/mmol) were purchased from PerkinElmer Life Sciences (Boston, MA). [3', 5', 7-^{3}H(N)]Methotrexate, disodium salt ([^{3}H]methotrexate, 23.0 Ci/mmol) was purchased from Moravek Biochemicals (Brea, CA). [1, 5-^{14}C]Glutarate (5.3 mCi/mmol) was purchased from American Radiolabeled Chemicals (St. Louis, MO). [ring-^{3}H]Indoxyl sulfate ([^{3}H]indoxyl sulfate, 6.5 Ci/mmol) was synthesized and purified by NEN Life Science Products. [ring-^{3}H]Homovanillic acid ([^{3}H]HVA, 12.5 Ci/mmol) was synthesized and purified by IZOTOP (Budapest, Hungary). PAH, probenecid, salicylic acid, benzylpenicillin potassium salt, cimetidine, indomethacin, 5-hydroxyindole-3-acetic acid, 3'-azido-3'-deoxythymidine, prostaglandin E_2, taurocholate sodium salt, pravastatin sodium salt, calcitonin acetate, α-naphthyl β-D-glucuronide and glutathione reduced form (GSH) were obtained from Wako Pure Chemical (Osaka, Japan). Homovanillic acid, sulfobromophthalein and uric acid were purchased from Nacalai Tesque (Kyoto, Japan). Indoxyl sulfate potassium salt, estrone-3-sulfate sodium salt, 1-hydroxyethane-1,1-diphosphonic acid (etidronic acid), parathyroid hormone, β–estradiol, tetraethylammonium, indoxyl β-D-glucuronide cyclohexylammonium

salt, β-estradiol 3-sulfate sodium salt, β-estradiol 3-sulfate 17-(β-D-glucuronide) dipotassium salt, 1-naphthyl β-D-glucuronide sodium salt, L-glutathione oxidized disodium salt (GSSG) and N-acethyl-S-farnesyl-L-cysteine methyl ester were purchased from Sigma Chemicals (St. Louis, MO). 3,5,3'-Triiodo-L-thyronine sodium salt and L-thyroxine sodium salt were purchased from Tokyo Kasei (Tokyo, Japan). Methotrexate was purchased from Calbiochem-Novabiochem (La Jolla, CA). All other chemicals were commercial products of analytical grade.

RT-PCR analysis and isolation of Roct cDNA

Total RNA was prepared from mouse tissues and brain capillary-rich fraction using TRIzol Reagent (Invitrogen, Carlsbad, CA). Isolation of the brain capillary-rich fraction was performed as described previously (Hosoya et al., 2000). Total RNA (1 μg) was reverse-transcribed with ReverTra Ace (Toyobo, Osaka, Japan). The synthesized cDNA was used for subsequent PCR. PCR primers for amplification of Roct cDNA were designed and synthesized based on the nucleotide sequence of Roct (Genbank accession number XM_123355). There was a sense strand with a *BamHI* site (underline), 5'-CGGGATCCCGGGTTCATCTTGCCTGGTGCCATG-3' (positions 63-85);

JPET Fast Forward. Published on February 4, 2004 as DOI: 10.1124/jpet.103.063370
This article has not been copyedited and formatted. The final version may differ from this version.

antisense with an *EcoRI* site (underline), 5'-CGGAATTCCGAAAGAGGATTCTGTTGTTCTTAGCTA-3' (positions 1694-1719). The amplification conditions were as follows: 94 °C for 30 s, 60 °C for 30 s, 74 °C for 60 s, for 30 cycles. The PCR products were separated by electrophoresis on 1% agarose gels. The RT-PCR product amplified from kidney was subcloned into the *EcoRV* site of pBluescript SKII(+) (Stratagene, LaJolla, CA) using a BKL kit (Takara, Shiga, Japan). Both strands of the subcloned cDNA inserts were subjected to DNA sequencing (model 4200, Li-COR) and cDNA clones with base sequences 100% identical to the coding region of Roct were isolated. Then, the Roct cDNA was cut out from pBluescript SKII(+)/Roct using *BamHI* and *EcoRI,* and subcloned into pGEM-HEN for *in vitro* transcription.

Functional Expression of Roct in *Xenopus laevis* Oocytes

Capped cRNA of Roct was transcribed from *NotI*-linearized pGEM-HEN containing Roct cDNA with T7 RNA polymerase as described previously (Deguchi et al., 2002). pGEM-HEN contains 3' and 5'UTR regions of *Xenopus* β-globin, which stabilize RNA and enhance the protein synthesis efficiency in the oocyte expression system (Liman et al., 1992). Defolliculated oocytes were

injected with 50 nL water or capped Roct cRNA (10 ng) and incubated in Barth's solution (88 mM NaCl, 1 mM KCl, 0.33 mM $Ca(NO_3)_2$, 0.4 mM $CaCl_2$, 0.8 mM $MgSO_4$, 2.4 mM $NaHCO_3$, and 10 mM HEPES) containing 50 μg/ml gentamicin and 2.5 mM pyruvate, pH 7.4, at 20°C. After incubation for 3 days, uptake experiments were performed.

Uptake by oocytes

The uptake experiment was initiated by replacing the ND96 solution (96 mM NaCl, 2 mM KCl, 1.8 mM $CaCl_2$, 1 mM $MgCl_2$, and 5 mM HEPES, pH 7.4) with one containing radiolabeled substrate and terminated by addition of ice-cold ND 96 solution after a 1 h incubation at 20°C. In previous studies employing OAT3-expressing oocytes, the uptake kinetics of [^{3}H]E_1S, [^{14}C]- or [^{3}H]PAH, [^{3}H]methotrexate and [^{3}H]cimetidine were determined at 1 h as well (Kusuhara et al., 1999; Cha et al., 2001), as was also the case in studies of [^{3}H]estradiol 17β-D-glucuronide, [^{3}H]indoxyl sulfate, [^{3}H]homovanillic acid, [^{14}C]glutarate and [^{14}C]salicylic acid uptake (Cha et al., 2001; Ohtsuki et al., 2002; Mori et al., 2003). The concentrations of radiolabeled substrates were different due to the differences in the specific radioactivity of substrates. Therefore, the transport

JPET Fast Forward. Published on February 4, 2004 as DOI: 10.1124/jpet.103.063370
This article has not been copyedited and formatted. The final version may differ from this version.

activity was normalized by substrate concentration and indicated in the unit of μL/(h·oocyte). Na^+-free ND96 solution was prepared by equimolar replacement of NaCl with choline chloride. In the case of Cl^--free ND96 solution, NaCl, KCl, $CaCl_2$ and $MgCl_2$ were replaced with equimolar sodium gluconate, potassium gluconate, calcium gluconate and magnesium gluconate, respectively. Oocytes were washed four times with ice-cold ND96 solution and solubilized in 5% SDS, and the accumulated radioactivity was determined in a liquid scintillation counter (LS-6500, Beckman Coulter, Fullerton, CA).

The kinetic parameters for the uptake of benzylpenicillin or E_1S by Roct were estimated from the following equation (1):

$$V = V_{max} \times C/(K_m + C) \text{ ---------- (1)}$$

where V is the uptake rate of the benzylpenicillin or E_1S (pmol/(h·oocyte)), C is the benzylpenicillin or E_1S concentration in the medium (μM), K_m is Michaelis-Menten constant (μM), and V_{max} is the maximum uptake rate (pmol/(h·oocyte)). To obtain the kinetic parameters, the equation was fitted to the Roct-specific transport rate, which was obtained by subtracting the transport rate in water-injected oocytes from that in Roct-expressing oocytes, by an iterative nonlinear least-squares method using the MULTI program (Yamaoka et al.,

1981). The input data were weighted as the reciprocal of the observed values, and the damping Gauss-Newton algorithm was used for fitting. The fitted line was converted to the V/C versus V form (Eadie-Scatchard plot).

For the inhibition study, uptake of 500 nM [^{3}H]benzylpencillin by Roct was measured in the presence or absence of unlabeled compounds in ND96 solution. The concentration of inhibitors was 1 mM in most cases. However, calcitonin was examined at 10 μM since this was the maximum concentration that could be prepared from 1 vial (200 μg), and triiodothyronine, thyroxine and estradiol were examined at 0.1 mM due to their low solubility. Parathyroid hormone was tested at 0.1 μM, since it was reported to have an inhibitory effect on phosphate transport at this concentration (Ba et al., 2003), and indoxyl glucuronide, estradiol sulfate, estradiol glucuronide sulfate, naphthyl sulfate, naphthyl glucuronide, GSSG, GSH and N-acetyl-S-farnesyl-cys were examined at 5 μM, since inhibitory effects of these conjugates were reported at this concentration in the case of OAT4 (Cha et al., 2000). The specific uptake was obtained by subtracting the uptake into water-injected oocytes from that into Roct-expressing oocytes.

For experiments involving co-expression of Roct and rat Na^+-dicarboxylate

JPET Fast Forward. Published on February 4, 2004 as DOI: 10.1124/jpet.103.063370
This article has not been copyedited and formatted. The final version may differ from this version.

cotransporter (rNaDC-1), rNaDC-1 cDNA was isolated from rat kidney by RT-PCR and inserted into pBluescript SKII(+). cRNA was synthesized from its cDNA using T3 RNA polymerase. rNaDC-1 cRNA injected oocytes exhibited significant uptake of [^{14}C]glutarate compared with that by water injected oocytes (0.108 ± 0.020 (μL/(h·oocyte)) and 0.0409 ± 0.0220 (μL/(h·oocyte)), respectively (p<0.01)). Roct and rNaDC-1 cRNA were co-injected at a ratio of 2:1. For trans-stimulation studies, oocytes were pretreated for 90 min with incubation in ND96 solution containing 100 μM glutarate or in Na^+-free ND96 solution containing 100 μM glutarate, and quickly washed four times with glutarate-free ice-cold ND96 solution before initiation of uptake.

Data analysis

Unless otherwise indicated, all data are presented as the mean ± S.E.M. An unpaired, two-tailed Student's *t* test was used to determine the significance of differences between two group means. One-way ANOVA followed by the modified Fisher's least-significant-difference method was used to assess the statistical significance of differences among means of more than two groups.

Northern blot analysis

Blots containing 2 μg aliquots of poly(A)$^+$ RNA from various mouse tissues (mouse multiple tissue Northern (MTN)^{TM} blot: CLONTECH, Palo Alto, CA) were hybridized with a cDNA fragment of Roct (corresponding to positions 557-1409) as a probe; this region encodes an amino acid sequence with 48% and 41% identity to the corresponding regions of mouse OAT1 and mouse OAT2, respectively. The filter was washed twice with 2 x SSC (1 x SSC = 0.15 M NaCl and 0.015 M sodium acetate) and 0.05% SDS for 30 min at room temperature, and then twice with 0.1 x SSC and 0.1% SDS for 40 min at 50°C. Then, the filter was exposed to film (X-OMAT, Kodak, Rochester, NY).

Western blot analysis

The membrane protein fraction of mouse brain, kidney and small intestine epithelium was prepared using the procedure described in a previous report (Hosoya et al., 2000). The protein (62.5 μg per lane) was subjected to SDS-polyacrylamide gel electrophoresis. The separated proteins were electrotransferred to nitrocellulose membrane (Toyo Roshi, Tokyo, Japan), and the membrane was treated with blocking solution (Block Ace; Dainihon

Pharmaceutical, Osaka, Japan) for 1 h at room temperature and diluted affinity-purified anti-OAT3 antibody (1 μg/ml) for 16 h at 4°C. Anti-OAT3 antibody was raised against an oligopeptide (KTKQESEAEKAS) corresponding to amino acid residues 516-527 of rOAT3 (Mori et al., 2003). Membranes were washed 5 times with 0.1% Tween20/phosphate-buffered saline (PBS) and then incubated with horseradish peroxidase-conjugated goat anti-rabbit IgG (1:5000; Kirkegaard & Perry Laboratories, Gaithersburg, MD) for 1 h at room temperature. Immunoreactivity was visualized with an enhanced chemiluminescence kit (Supersignal west pico chemiluminescent substrate; Pierce, Rockford, IL).

Immunostaining analysis

Adult mice were anesthetized with an intramuscular injection of ketamine and xylazine before perfusion through the carotid artery with 2% paraformaldehyde in 0.1 M phosphate buffer. The cerebrum was excised and immersed in 0.5 M sucrose/0.1 M phosphate buffer solution. Sagittal sections (10-μm thick) were cut from the frozen cerebrum using a cryostat (CM1900; Leica, Heidelberg, Germany) and mounted on silanized slide glasses (DAKO, Carpinteria, MA). The sections were incubated with 10% goat serum (Histofine; Nichirei, Tokyo, Japan)

for 1 h at room temperature. The primary antibody (1 μg/mL rabbit anti-Roct antibody or 3.1 μg/mL mouse anti-GFAP (glial fibrillary acidic protein) antibody (Sigma)) was applied to the sections, which were incubated for 2 nights at 4°C. For single staining of Roct, sections were further incubated with Alexa 488-conjugated goat anti-rabbit IgG (1:200; Molecular Probes, Eugene, OR) as a secondary antibody. For double staining, Alexa 546-conjugated goat anti-mouse IgG (1:200; Molecular Probes) was used as a secondary antibody for anti-GFAP antibody. Sections were mounted using “Vectashield” mounting medium (Vector Laboratories, Burlingame, CA). The stained sections were viewed using a confocal laser microscope (TCS SP; Leica, Heidelberg, Germany).

Results

Roct transports substrates of OAT3

Roct cDNA was isolated from mouse kidney. The oocytes injected with Roct cRNA exhibited 118-fold greater [^{3}H]PAH uptake than water-injected oocytes (Table 1), indicating that Roct is a PAH transporter, like the OAT family. Roct cRNA-injected oocytes exhibited uptake of various OAT3 substrates, such as [^{3}H]E_1S, [^{3}H]benzylpenicillin, [^{3}H]estradiol 17β-glucronide, [^{3}H]indoxyl sulfate and [^{3}H]cimetidine. Furthermore, [^{14}C]indomethacin, [^{3}H]homovanillic acid, [^{14}C]glutarate, [^{14}C]salicylic acid and [^{3}H]methotrexate were taken up by the cRNA-injected oocytes. In contrast, [^{3}H]digoxin, which is a substrate of organic anion transporting polypeptide 2 (oatp2; SLC21A5), but not of OAT family members, was not taken up by the cRNA-injected oocytes. These results indicate that Roct mediates transport of OAT3 substrates and other organic anions.

Transport properties of Roct-mediated uptake of benzylpenicillin and E_1S.

The uptake of [^{3}H]benzylpenicillin and [^{3}H]E_1S by Roct cRNA-injected oocytes increased linearly for about 120 min (Fig. 1). Accordingly, analysis was

carried out at 60 min in the following uptake study. As shown in Fig. 2, benzylpenicillin and E_1S uptake was concentration-dependent. The K_m and V_{max} values of benzylpenicillin uptake were obtained as 40.0 ± 7.8 μM and 42.8 ± 5.4 pmol/(h·oocyte), respectively (mean ± SD), and those of E_1S were found to be 5.54 ± 1.59 μM and 15.2 ± 1.8 pmol/(h·oocyte), respectively (mean ± SD). Under Na^+-free and Cl^--free conditions, the [^{3}H]benzylpenicillin uptake by Roct was 82.5 ± 9.0 % and 69.0 ± 11 % of the control, respectively, and the values are not significantly different from the control.

Trans-stimulation effect of glutarate on the uptake by Roct was examined by using oocytes co-expressing Roct and rat NaDC-1 (Fig. 3). Glutarate preloading increased the uptakes of benzylpenicillin and E_1S by 1.40- and 1.38-fold, respectively, compared with the uptake without glutarate, although these changes are not statistically significant. Na^+-free conditions significantly reduced the stimulation of benzylpenicillin uptake by glutarate preloading ($p<0.05$), and the stimulation of E_1S uptake was also reduced, although without statistical significance.

Inhibitory effects of various compounds on benzylpenicillin uptake

JPET Fast Forward. Published on February 4, 2004 as DOI: 10.1124/jpet.103.063370
This article has not been copyedited and formatted. The final version may differ from this version.

mediated by Roct

To investigate the substrate selectivity of Roct, the cis-inhibitory effect of various compounds on Roct-mediated [^{3}H]benzylpenicillin uptake was examined (Table 2). OAT3 substrates and inhibitors, such as probenecid, PAH, sulfobromophthalein, taurocholate, cimetidine, indomethacin, homovanillic acid, salicylic acid, methotrexate, 3'-azido-3'-deoxythymidine, 5-hydroxyindole-3-acetic acid, pravastatin and uric acid exhibited distinct inhibitory potency. In contrast, tetraethylammonium, which is a substrate of organic cation transporter (OCT), did not significantly affect the uptake. Among the compounds involved in bone turnover, prostaglandin E_2 and triiodothyronine inhibited the uptake, whereas thyroxine, etidronic acid, calcitonin, parathyroid hormone and estradiol had no significant effect.

The inhibitory effect of conjugated compounds was also examined (Table 3). Sulfate conjugated estrone, indoxyl and estradiol inhibited the uptake activity, and indoxyl glucuronide and estradiol glucuronide sulfate also exhibited a significant inhibitory effect. In contrast, naphthyl sulfate, naphtyl glucuronide, two forms of glutathione (GSSG and GSH), and N-acetyl-S-farnesyl-cys did not affect the uptake by Roct significantly.

Distribution of Roct mRNA in mouse tissues

Expression of Roct mRNA in mouse tissues was examined by Northern blot analysis (Fig. 4A). A strong 2.7-kb band was detected in the kidney. A similar, but faint, band was also detected in the brain, but not in the heart, spleen, lung, liver, skeletal muscle or testis. The DNA probe used in this Northern blot hybridized to Roct with at least 100-fold greater affinity than to rOAT1 and rOAT2 in dot blot analysis, suggesting that the probe selectively detected Roct (data not shown). Further RT-PCR analysis showed that Roct mRNA was detected in the brain, brain capillary-rich fraction, kidney, eye and choroid plexus at the expected size (1653 bp), whereas no such band was detected in the liver or small intestine (Fig. 4B).

Localization of Roct in mouse brain capillaries

Cross-reactivity of anti-OAT3 polyclonal antibody was evaluated by Western blot analysis, since the antigen peptide for this antibody (KTKQESEAEKAS) is only one amino acid different from the corresponding peptide in Roct (KTKQEPEAEKAS). As shown in Fig. 5, a band was detected in crude

membrane fraction of mouse kidney and brain at 50 kDa, which is the same size as reported in the rat kidney, brain and brain capillary-rich fraction and in rOAT3-expressing LLC-PK1 cells (Hasegawa et al., 2002; Mori et al., 2003). This band was not detected in the crude membrane fraction of mouse small intestine. Therefore, this antibody was suggested to react selectively with Roct in mouse brain, including brain capillaries.

The result of the immunohistochemical analysis of Roct in mouse brain capillaries is shown in Fig. 6. Immunoreactivity of GFAP, an astrocyte marker, surrounds the brain blood vessels (Figs. 6B, E and H; red), and Roct immunoreactivity is observed inside the GFAP signals (Figs. 6C, F and I; green). Roct immunoreactivity was observed not only in relatively large blood vessels (Figs. 6A and D), but also in capillaries (Fig 6G). No significant fluorescence was observed in brain blood vessels with normal rabbit IgG (data not shown). Figure 6K shows the result of propidium iodide staining of nuclei (red) in capillary endothelial cells. Roct (green) is localized outside the nuclei (Fig. 6L). These results suggest that Roct is localized at the abluminal membrane of brain capillary endothelial cells.

Discussion

The Roct gene encodes a protein that has high amino acid sequence homology with rOAT3 (92.4%) and hOAT3 (78.0%). However, Roct also has 35% to 49% homology with OAT1 (SLC22A6), OAT2 (SLC22A7), OAT4 (SLC22A11) and OAT5 (SLC22A10), and it has not been investigated in detail whether Roct functions as mouse OAT3.

In this study we have clarified the transport properties of Roct. Roct mediates transport of compounds which have been reported to be transported by rOAT3 and/or hOAT3 (Table 1) (Kusuhara et al., 1999; Cha et al., 2001; Deguchi et al., 2002; Hasegawa et al., 2003; Mori et al., 2003). Roct-expressing oocytes exhibited uptake of benzylpenicillin with K_m value of 40.0 μM (Figs. 2A) and in an Na^+-independent manner, like that by rOAT3 (K_m = 85.1 μM) (Kusuhara et al., 1999; Hasegawa et al., 2003), and there was no significant effect under Cl^--free conditions. The K_m value of E_1S uptake by Roct was 5.54 μM (Fig. 2B), which is close to that of rOAT3 and hOAT3 (2.3 μM and 3.1 μM, respectively) (Kusuhara et al., 1999; Cha et al., 2001). rOAT3 has been reported to be a dicarboxylate exchanger (Sweet et al., 2003). The uptake of [^{3}H]benzylpenicillin and [^{3}H]E_1S appeared to be trans-stimulated by glutarate

preloading with co-expression of rNaDC-1 (Fig. 3), suggesting that Roct is a dicarboxyl exchanger like rOAT3. [^{3}H]Benzylpenicillin uptake by Roct was also inhibited by various compounds in a similar manner to that by rOAT3 and hOAT3 (Table 2) (Kusuhara et al., 1999; Cha et al., 2001). While partial degradation of the radiolabeled compounds during uptake can not be ruled out, the properties exhibited by Roct-expressing oocytes were similar to those of rat and/or human OAT-expressing oocytes. Therefore, these transport properties suggest that Roct functions as mouse OAT3.

Compared with the transport properties of other organic ion transporters, Roct transported estradiol 17β-glucronide (Table 1), and this compound was transported by rOAT3 but not by rOAT1 (Sugiyama et al., 2001). The uptake by Roct was inhibited by indoxyl sulfate (Table 2), which does not inhibit prostaglandin $F_{2\alpha}$ uptake by rOAT2 (Enomoto et al., 2003). Digoxin is a substrate of rat oatp2 (Sugiyama et al., 2001), although Roct did not transport it (Table 1). The OCT family forms a part of the organic ion transporter superfamily (SLC22) with the OAT family, but an OCT substrate, tetraethylammonium, did not affect the uptake by Roct. These results are consistent with the idea that Roct acts as mouse OAT3.

JPET Fast Forward. Published on February 4, 2004 as DOI: 10.1124/jpet.103.063370
This article has not been copyedited and formatted. The final version may differ from this version.

Despite the similarity in the properties of rOAT3 and hOAT3, there are some differences in their transport properties and tissue expression. The transport properties of Roct resemble those of hOAT3 rather than rOAT3. [^{3}H]E_1S uptake by rOAT3 was not inhibited by 1 mM indomethacin (Kusuhara et al., 1999). In contrast, the uptakes by hOAT3 and Roct were strongly inhibited by indomethacin (Table 2) (Cha et al., 2001), and Roct exhibited significant uptake of [^{3}H]indomethacin (Table 1). Furthermore, the tissue distribution of Roct is similar to that of hOAT3. rOAT3 is expressed in liver (Kusuhara et al., 1999), whereas mRNAs of Roct and hOAT3 were not detected (Fig. 4) (Cha et al., 2001). Taking these results into consideration, we conclude that Roct functions as mouse OAT3, and its properties are similar to those of hOAT3 rather than rOAT3.

Roct is expressed in the kidney (Fig. 4), and the uptake of PAH, E_1S and taurocholate by renal slices is decreased in Roct-knockout mouse compared with the wild type (Sweet et al., 2002), suggesting that Roct plays a certain role in the kidney. Recently, Jutabha et al. (2003) identified OATv1 and proposed the renal excretion pathway, in which organic anions are taken up by the epithelial cells via OAT1 and OAT3 and exit from the cells via OATv1. The uptake activity

by OATv1 was inhibited by various sulfate and glucuronide conjugates, whereas there was little information about the substrate specificity of OAT3/Roct as far as conjugates are concerned. The uptake by Roct was inhibited by sulfate and glucuronide conjugates (Table 3), and, among those, E_1S, indoxyl sulfate, indoxyl glucuronide and estradiol sulfate inhibited both Roct and OATv1 transport, while glutathiones and a cysteine conjugate did not inhibit the uptake. These results suggest that OAT3/Roct accepts sulfate and glucuronide conjugates as a substrate, and is likely to be involved in renal excretion of those conjugates cooperating with OATv1.

Chronic renal failure is often associated with bone disease. One possible explanation is that OAT3/Roct is involved in the renal excretion of hormones related to bone turnover, and impairment of OAT3/Roct functions alters the plasma level of those hormones, resulting in a changing in bone turnover rate. In fact, E_1S, a metabolite of estrone, is a high-affinity substrate of Roct and OAT3 (Fig. 2B) (Kusuhara et al., 1999; Cha et al., 2001), and estrogens regulate bone formation and resorption. Moreover, the plasma level of estrone in postmenopausal women is correlated with bone mineral density (Takayanagi et al., 2002). However, the transport properties of OAT3/Roct have not been

investigated in relation to bone turnover. In the present study, the inhibitory effect of compounds related to bone turnover was investigated (Table 2). Etidronic acid is a drug used to treat osteoporosis. Calcitonin and estradiol promote osteogenesis. Prostaglandin E_2, parathyroid hormone and thyroid hormones influence the differentiation of osteoclasts (Katagiri and Takahashi, 2002). Among these compounds, prostaglandin E_2 and triiodothyronine inhibited the uptake (Table 2). Therefore, alteration in the transport of these hormones in the body is likely to influence bone turnover in renal failure patients and the *oc* mutant mouse.

Calcitonin and GSH increased the uptake by Roct by 52% and 40%, respectively (Tables 2 and 3). One possible explanation is that calcitonin and GSH increased the uptake by functioning as a driving force. The other is that the activity of Roct was promoted by modification, such as phosphorylation. Roct has 8 putative protein kinase C phosphorylation sites, and calcitonin activates the protein kinase C pathway (Kajiya et al., 2003), while the effect of phosphorylation on OAT3/Roct is still unknown.

Our recent reports have shown that rOAT3 is expressed at the BBB and is involved in the efflux transport of uremic toxins and neurotransmitter metabolites

from the brain (Ohtsuki et al., 2002; Mori et al., 2003). The present study shows that Roct is expressed at brain capillary endothelial cells (Figs. 4B and 6). Luminal and abluminal membranes are separated by only 0.1-0.2 μm and it is difficult to distinguish between them, while they diverge to surround the endothelial nucleus and are separated sufficiently (approximately 1-2 μm) to be resolved under confocal microscopy (Stewart et al., 1996). Therefore, the signal between GFAP and endothelial nuclei suggests that Roct is localized at the abluminal membrane of capillary endothelial cells (Fig. 6). Further study by using an astrocyte foot process marker, such as aquaporin-4 (Simard et al., 2003), and analysis with electron microscopy are necessary to establish precisely the abluminal localization of Roct, since there are difficulties in differentiating endothelial abluminal membrane from astrocyte or pericyte membrane.

rOAT3 is expressed in choroid plexus and is involved in the cerebrospinal fluid (CSF)-to-blood transport at the blood-cerebrospinal fluid barrier (BCSFB) (Nagata et al., 2002). Similarly, Roct is expressed in choroid plexus (Fig. 4B), and Roct knock-out mouse showed a decreased accumulation of fluorescein in capillaries from CSF, compared with that of the wild type (Sweet et al., 2002). Roct mediates the transport of a uremic toxin, indoxyl sulfate, and a dopamine

metabolite, homovanillic acid, and its activity was inhibited by a serotonin metabolite, 5-hydroxyindole-3-acetic acid (Tables 1 and 2). Therefore, Roct is suggested to be involved in the clearance system for uremic toxins and neurotransmitter metabolites from the brain and CSF in mouse.

OAT3/Roct and V-ATPase genes are located in the same genomic locus in both human and mouse (Heaney et al., 1998; Scimeca et al., 2000; Cha et al., 2001). In mouse, suppression of the V-ATPase gene would influence Roct expression, since deletion of only the V-ATPase gene has been reported in the *oc* mutant (Scimeca et al., 2000). Therefore, in humans, it is conceivable that mutation in the V-ATPase gene influences the expression of hOAT3, since the genomic locations of these genes are conserved between human (ch11q11-13) and mouse (Chr 19) (Hudson et al., 2001). A reduction of OAT3/Roct expression would change the levels of substrate compounds in the blood and brain and this change could, in part, be associated with phenotypes such as osteopetrosis and neural defect.

In conclusion, the present study shows that Roct functions as mouse OAT3, and we suggest that it transports not only sulfate conjugates, but also glucuronide conjugates. Therefore, Roct is likely to be involved in the

brain-to-blood BBB efflux transport and renal excretion of various compounds, including uremic toxins, neurotransmitter metabolites and conjugates. Furthermore, Roct interacts with compounds involved in bone turnover, such as E_1S, prostaglandin E_2 and triiodothyronine. These results provide important information to allow a better understanding of the physiological role of OAT3/Roct at the BBB, BCSFB and kidney.

Acknowledgments

We would like to thank Dr. Abe for kindly supplying the pGEM-HEN vector for heterogeneous protein expression in *Xenopus laevis* oocytes, Mr. T. Deguchi for technical assistance and Ms. N. Funayama for secretarial assistance.

References

Adams JE (2002) Dialysis bone disease. *Semin Dial* **15**:277-289.

Ba J, Brown D and Friedman PA (2003) Calcium-sensing receptor regulation of PTH-inhibitable proximal tubule phosphate transport. *Am J Physiol Renal Physiol* **285**:F1233-1243.

Brady KP, Dushkin H, Fornzler D, Koike T, Magner F, Her H, Gullans S, Segre GV, Green RM and Beier DR (1999) A novel putative transporter maps to the osteosclerosis (oc) mutation and is not expressed in the oc mutant mouse. *Genomics* **56**:254-261.

Cha SH, Sekine T, Fukushima JI, Kanai Y, Kobayashi Y, Goya T and Endou H (2001) Identification and characterization of human organic anion transporter 3 expressing predominantly in the kidney. *Mol Pharmacol* **59**:1277-1286.

Cha SH, Sekine T, Kusuhara H, Yu E, Kim JY, Kim DK, Sugiyama Y, Kanai Y and Endou H (2000) Molecular cloning and characterization of multispecific organic anion transporter 4 expressed in the placenta. *J Biol Chem* **275**:4507-4512.

Deguchi T, Ohtsuki S, Otagiri M, Takanaga H, Asaba H, Mori S and Terasaki T

(2002) Major role of organic anion transporter 3 in the transport of indoxyl sulfate in the kidney. *Kidney Int* **61**:1760-1768.

Enomoto A, Takeda M, Taki K, Takayama F, Noshiro R, Niwa T and Endou H (2003) Interactions of human organic anion as well as cation transporters with indoxyl sulfate. *Eur J Pharmacol* **466**:13-20.

Goldin AL (1992) Maintenance of Xenopus laevis and oocyte injection. *Methods Enzymol* **207**:226-279.

Hasegawa M, Kusuhara H, Endou H and Sugiyama Y (2003) Contribution of organic anion transporters to the renal uptake of anionic compounds and nucleoside derivatives in rat. *J Pharmacol Exp Ther* **305**:1087-1097.

Hasegawa M, Kusuhara H, Sugiyama D, Ito K, Ueda S, Endou H and Sugiyama Y (2002) Functional involvement of rat organic anion transporter 3 (rOat3; Slc22a8) in the renal uptake of organic anions. *J Pharmacol Exp Ther* **300**:746-753.

Heaney C, Shalev H, Elbedour K, Carmi R, Staack JB, Sheffield VC and Beier DR (1998) Human autosomal recessive osteopetrosis maps to 11q13, a position predicted by comparative mapping of the murine osteosclerosis (oc) mutation. *Hum Mol Genet* **7**:1407-1410.

Hosoya K, Tetsuka K, Nagase K, Tomi M, Saeki S, Ohtsuki S, Takanaga H, Yanai N, Obinata M, Kikuchi A, Okano T and Terasaki T (2000) Conditionally immortalized brain capillary endothelial cell lines established from a transgenic mouse harboring temperature-sensitive simian virus 40 large T-antigen gene. *AAPS PharmSci* **2**:E27.

Hudson TJ, Church DM, Greenaway S, Nguyen H, Cook A, Steen RG, Van Etten WJ, Castle AB, Strivens MA, Trickett P, Heuston C, Davison C, Southwell A, Hardisty R, Varela-Carver A, Haynes AR, Rodriguez-Tome P, Doi H, Ko MS, Pontius J, Schriml L, Wagner L, Maglott D, Brown SD, Lander ES, Schuler G and Denny P (2001) A radiation hybrid map of mouse genes. *Nat Genet* **29**:201-205.

Jutabha P, Kanai Y, Hosoyamada M, Chairoungdua A, Kim do K, Iribe Y, Babu E, Kim JY, Anzai N, Chatsudthipong V and Endou H (2003) Identification of a novel voltage-driven organic anion transporter present at apical membrane of renal proximal tubule. *J Biol Chem* **278**:27930-27938.

Kajiya H, Okamoto F, Fukushima H and Okabe K (2003) Calcitonin inhibits proton extrusion in resorbing rat osteoclasts via protein kinase A. *Pflugers Arch* **445**:651-658.

Katagiri T and Takahashi N (2002) Regulatory mechanisms of osteoblast and osteoclast differentiation. *Oral Dis* **8**:147-159.

Kusuhara H, Sekine T, Utsunomiya-Tate N, Tsuda M, Kojima R, Cha SH, Sugiyama Y, Kanai Y and Endou H (1999) Molecular cloning and characterization of a new multispecific organic anion transporter from rat brain. *J Biol Chem* **274**:13675-13680.

Liman ER, Tytgat J and Hess P (1992) Subunit stoichiometry of a mammalian K^+ channel determined by construction of multimeric cDNAs. *Neuron* **9**:861-871.

Mori S, Takanaga H, Ohtsuki S, Deguchi T, Kang YS, Hosoya K and Terasaki T (2003) Rat organic anion transporter 3 (rOAT3) is responsible for brain-to-blood efflux of homovanillic acid at the abluminal membrane of brain capillary endothelial cells. *J Cereb Blood Flow Metab* **23**:432-440.

Nagata Y, Kusuhara H, Endou H and Sugiyama Y (2002) Expression and functional characterization of rat organic anion transporter 3 (rOat3) in the choroid plexus. *Mol Pharmacol* **61**:982-988.

Ohtsuki S, Asaba H, Takanaga H, Deguchi T, Hosoya K, Otagiri M and Terasaki T (2002) Role of blood-brain barrier organic anion transporter 3 (OAT3) in

the efflux of indoxyl sulfate, a uremic toxin: its involvement in neurotransmitter metabolite clearance from the brain. *J Neurochem* **83**:57-66.

Scimeca JC, Franchi A, Trojani C, Parrinello H, Grosgeorge J, Robert C, Jaillon O, Poirier C, Gaudray P and Carle GF (2000) The gene encoding the mouse homologue of the human osteoclast-specific 116-kDa V-ATPase subunit bears a deletion in osteosclerotic (oc/oc) mutants. *Bone* **26**:207-213.

Simard M, Arcuino G, Takano T, Liu QS and Nedergaard M (2003) Signaling at the gliovascular interface. *J Neurosci* **23**:9254-9262.

Sobacchi C, Frattini A, Orchard P, Porras O, Tezcan I, Andolina M, Babul-Hirji R, Baric I, Canham N, Chitayat D, Dupuis-Girod S, Ellis I, Etzioni A, Fasth A, Fisher A, Gerritsen B, Gulino V, Horwitz E, Klamroth V, Lanino E, Mirolo M, Musio A, Matthijs G, Nonomaya S, Notarangelo LD, Ochs HD, Superti Furga A, Valiaho J, van Hove JL, Vihinen M, Vujic D, Vezzoni P and Villa A (2001) The mutational spectrum of human malignant autosomal recessive osteopetrosis. *Hum Mol Genet* **10**:1767-1773.

Stewart PA, Beliveau R and Rogers KA (1996) Cellular localization of

P-glycoprotein in brain versus gonadal capillaries. *J Histochem Cytochem* **44**:679-685.

Sugiyama D, Kusuhara H, Shitara Y, Abe T, Meier PJ, Sekine T, Endou H, Suzuki H and Sugiyama Y (2001) Characterization of the efflux transport of 17β-estradiol-D-17β-glucuronide from the brain across the blood-brain barrier. *J Pharmacol Exp Ther* **298**:316-322.

Sweet DH, Chan LM, Walden R, Yang XP, Miller DS and Pritchard JB (2003) Organic anion transporter 3 (Slc22a8) is a dicarboxylate exchanger indirectly coupled to the Na^+ gradient. *Am J Physiol Renal Physiol* **284**:F763-769.

Sweet DH, Miller DS, Pritchard JB, Fujiwara Y, Beier DR and Nigam SK (2002) Impaired organic anion transport in kidney and choroid plexus of organic anion transporter 3 (Oat3 (Slc22a8)) knockout mice. *J Biol Chem* **277**:26934-26943.

Takayanagi R, Goto K, Suzuki S, Tanaka S, Shimoda S and Nawata H (2002) Dehydroepiandrosterone (DHEA) as a possible source for estrogen formation in bone cells: correlation between bone mineral density and serum DHEA-sulfate concentration in postmenopausal women, and the

presence of aromatase to be enhanced by 1,25-dihydroxyvitamin D3 in human osteoblasts. *Mech Ageing Dev* **123**:1107-1114.

Yamaoka K, Tanigawara Y, Nakagawa T and Uno T (1981) A pharmacokinetic analysis program (multi) for microcomputer. *J Pharmacobiodyn* **4**:879-885.

Footnotes

This study was supported in part by a Grant-in-Aid for Scientific Research and a 21st Century Center of Excellence (COE) Program from the Japan Society for the Promotion of Science, Japan. It was also supported in part by the Industrial Technology Research Grant Program from the New Energy and Industrial Technology Development Organization (NEDO) of Japan.

Send reprint request to:

Professor Tetsuya Terasaki

Department of Molecular Biopharmacy and Genetics, Graduate School of Pharmaceutical Sciences, Tohoku University, Aoba, Aramaki, Aoba-ku, Sendai 980-8578, Japan

Voice: +81-22-217-6831; FAX: +81-22-217-6886

E-mail: terasaki@mail.pharm.tohoku.ac.jp

Table 1 Uptake of various ^{3}H- or ^{14}C-labeled compounds by Roct-expressing oocytes.

Tracer	Concentration (μM)	Water-injected (μl/(h·oocyte))	Roct cRNA-injected (μl/(h·oocyte))	Roct dependent (μl/(h·oocyte))
[^{3}H]E_1S	0.039	0. 0422 ± 0.0040	1.92 ± 0.20 **	1.88
[^{3}H]PAH	3.3	0. 0688 x 10^{-1} ± 0.0144 x 10^{-1}	8.16 x 10^{-1} ± 2.13 x 10^{-1} **	8.09 x 10^{-1}
[^{3}H]Benzylpenicillin	0.50	0.249 x 10^{-1} ± 0.058 x 10^{-1}	8.28 x 10^{-1} ± 0.87 x 10^{-1} **	8.03 x 10^{-1}
[^{3}H]Estradiol 17β-glucronide	0.039	0.429 x 10^{-1} ± 0.062 x 10^{-1}	7.26 x 10^{-1} ± 1.39 x 10^{-1} **	6.86 x 10^{-1}
[^{3}H]Indoxyl sulfate	2.0	0.405 x 10^{-1} ± 0.064 x 10^{-1}	5.55 x 10^{-1} ± 1.06 x 10^{-1} **	5.15 x 10^{-1}
[^{14}C]Indomethacin	7.5	0.637 ± 0.042	1.10 ± 0.21 *	4.67 x 10^{-1}
[^{3}H]Homovanillic acid	0.20	1.60 x 10^{-1} ± 0.17 x 10^{-1}	5.39 x 10^{-1} ± 1.47 x 10^{-1} **	3.79 x 10^{-1}
[^{3}H]Cimetidine	0.18	1.70 x 10^{-1} ± 0.28 x 10^{-1}	4.77 x 10^{-1} ± 1.11 x 10^{-1} *	3.07 x 10^{-1}
[^{14}C]Glutarate	129	0.115 x 10^{-1} ± 0.013 x 10^{-1}	1.84 x 10^{-1} ± 0.19 x 10^{-1} **	1.73 x 10^{-1}
[^{14}C]Salicylic acid	2.4	4.07 x 10^{-1} ± 0.23 x 10^{-1}	5.13 x 10^{-1} ± 0.29 x 10^{-1} *	1.06 x 10^{-1}
[^{3}H]Methotrexate	0.63	0.892 x 10^{-2} ± 0.065 x 10^{-2}	9.75 x 10^{-2} ± 3.28 x 10^{-2} *	8.86 x 10^{-2}
[^{3}H]Digoxin	0.59	7.59 x 10^{-2} ± 0.77 x 10^{-2}	9.48 x 10^{-2} ± 0.80 x 10^{-2}	N.S.

The uptake of radiolabeled compounds by the water-injected oocytes (control) or Roct cRNA-injected oocytes (Roct) was measured at 1 h. Roct-dependent uptake was calculated by subtracting the uptake by water-injected oocytes from that by Roct cRNA-injected oocytes. Each value represents the mean ± S.E.M. of 5-13 oocytes. *$p < 0.05$, **$p < 0.01$ significantly different from the uptake by water-injected oocytes. N.S.: Not significantly different.

JPET Fast Forward. Published on February 4, 2004 as DOI: 10.1124/jpet.103.063370
This article has not been copyedited and formatted. The final version may differ from this version.

Table 2 Effect of various compounds on [^{3}H]benzylpenicillin uptake by Roct

Inhibitors	Number of Investigations	% of control
Control	67	100 ± 6.5
Control[1]	22	100 ± 13
OAT3 substrates and/or inhibitors		
Probenecid	10	0.625 ± 0.30*
PAH	9	14.2 ± 6.9*
Sulfobromophthalein	10	2.54 ± 0.077*
Taurocholate	9	19.5 ± 7.4*
Cimetidine	8	6.88 ± 3.3*
Indomethacin	10	1.32 ± 0.18*
Homovanillic acid	10	40.9 ± 8.1*
Salicylic acid	10	11.4 ± 0.87*
Methotrexate	22	48.4 ± 9.8*
3'-Azido-3'-deoxythymidine	11	5.13 ± 0.54*
5-Hydroxyindole-3-acetic acid	10	21.7 ± 2.2*
Pravastatin	18	2.85 ± 0.42*
Uric acid	10	19.9 ± 1.8*
OCT substrate		
Tetraethylammonium	10	87.9 ± 18
Compounds involved in bone turnover		
Prostaglandin E_2	12	0.101 ± 0.049*
Triiodothyronine (T_3)[1]	24	39.8 ± 4.7*
Thyroxin (T_4)[1]	24	83.5 ± 9.1
Etidronic acid	27	118 ± 14
Calcitonin	10	152 ± 27*
Parathyroid hormone	13	89.9 ± 21
Estradiol[1]	25	115 ± 15

The uptake of [^{3}H]benzylpenicillin (500 nM) was measured at 1 h in the absence (control) or presence of 1 mM inhibitors except for the following: 10 μM calcitonin,

0.1 μM parathyroid hormone, 0.1 mM triiodothyronine, 0.1 mM thyroxin and 0.1 mM estradiol. Roct-mediated transport was obtained by subtracting the uptake rate in water-injected oocytes from that in Roct-expressing oocytes. Each value represents the mean ± S.E.M. *$p < 0.01$ significantly different from control.

[1] The uptake was performed in ND96 buffer containing 0.1% DMSO.

JPET Fast Forward. Published on February 4, 2004 as DOI: 10.1124/jpet.103.063370
This article has not been copyedited and formatted. The final version may differ from this version.

Table 3 Effect of conjugated compounds on [^{3}H]benzylpenicillin uptake by Roct

Inhibitors	Number of Investigations	% of control
Control	40	100 ± 6.1
E_1S	9	11.4 ± 6.7*
Indoxyl sulfate	7	21.9 ± 12.9*
Indoxyl glucuronide	10	72.3 ± 12.1*
Estradiol sulfate	12	65.5 ± 7.5*
Estradiol glucuronide sulfate	10	62.4 ± 10.4*
Naphthyl sulfate	10	107 ± 23
Naphthyl gulcuronide	11	101 ± 18
GSSG	11	98.3 ± 14.1
GSH	8	140 ± 21*
N-acethyl-S-farnesyl-cys	10	103 ± 13

The uptake of [^{3}H]benzylpenicillin (500 nM) was measured at 1 h in the absence (control) or presence of 5 μM inhibitors except for the following: 1 mM E_1S and 1 mM indoxyl sulfate. Roct-mediated transport was obtained by subtracting the uptake rate in water-injected oocytes from that in Roct-expressing oocytes. Each value represents the mean ± S.E.M. *$p < 0.01$ significantly different from control.

JPET Fast Forward. Published on February 4, 2004 as DOI: 10.1124/jpet.103.063370
This article has not been copyedited and formatted. The final version may differ from this version.

Figure Legends

Fig. 1 Time-courses of [^{3}H]benzylpenicillin and [^{3}H]E_1S uptake by water- or Roct cRNA-injected oocytes. The uptake of 500 nM [^{3}H]benzylpenicillin (A) or 39 nM [^{3}H]E_1S (B) in water-injected oocytes (open circle and square) and Roct-expressing oocytes (closed circle and square) were measured during a 180-min incubation. Each value represents the mean ± S.E.M. (n=5-12).

Fig. 2 Concentration-dependence of Roct-mediated uptake of benzylpenicillin (A) and E_1S (B). The uptake of [^{3}H]benzylpenicillin and [^{3}H]E_1S by water-injected or Roct-expressing oocytes was measured at the indicated concentration after incubation for 1 h. Roct-mediated transport was obtained by subtracting the transport rate in water-injected oocytes from that in Roct-expressing oocytes. Each value represents the mean ±S.E.M. (n=8-13).

Fig. 3. Trans-stimulation of Roct-mediated uptake of benzylpenicillin (A) and E_1S (B). The uptake of [^{3}H]benzylpenicillin and [^{3}H]E_1S was measured in oocytes co-injected with Roct and NaDC-1 cRNA. Oocytes were preloaded with 100 μM glutarate (Glutarate (+)) or without (Glutarate (-), control). Effects of Na^+-free

conditions (Na^+ (-)) during the preloading period were also assessed. Each value represents the mean ±S.E.M. (n=10-14). *p<0.05, significantly different from glutarate-stimulated uptake.

Fig. 4 Tissue distribution of Roct mRNA. A: Northern blot analysis. Two micrograms of poly $(A)^+$ RNA from various mouse tissues was used. The filter was hybridized with a probe for Roct (upper panel) or β-actin (lower panel). B: RT-PCR analysis. Total RNA was prepared from the indicated mouse tissues and analyzed by RT-PCR using specific primer sets for Roct (upper panel) and β-actin (lower panel). B. cap: brain capillary-rich fraction.

Fig. 5 Western blot analysis of Roct in mouse kidney, small intestine and brain. Crude membrane fractions of mouse kidney, small intestine and brain were subjected to SDS-PAGE. The transferred filter was reacted with anti-OAT3 antibody. Molecular weight markers are indicated on the left side.

Fig. 6 Localization of Roct at mouse brain capillary endothelial cells.

A-I: Brain sections (10-μm thick) were double-reacted with anti-OAT3 antibody

(A, D and G; green) and anti-GFAP antibody (B, E and H; red), and the images were overlaid (C, F and I). J-L: Immunostaining of brain section with anti-OAT3 antibody (J; green), and nuclear staining with propidium iodide (K; red). The images were overlaid (L). Bar; 20 μm (A-F), 2 μm (G-L)

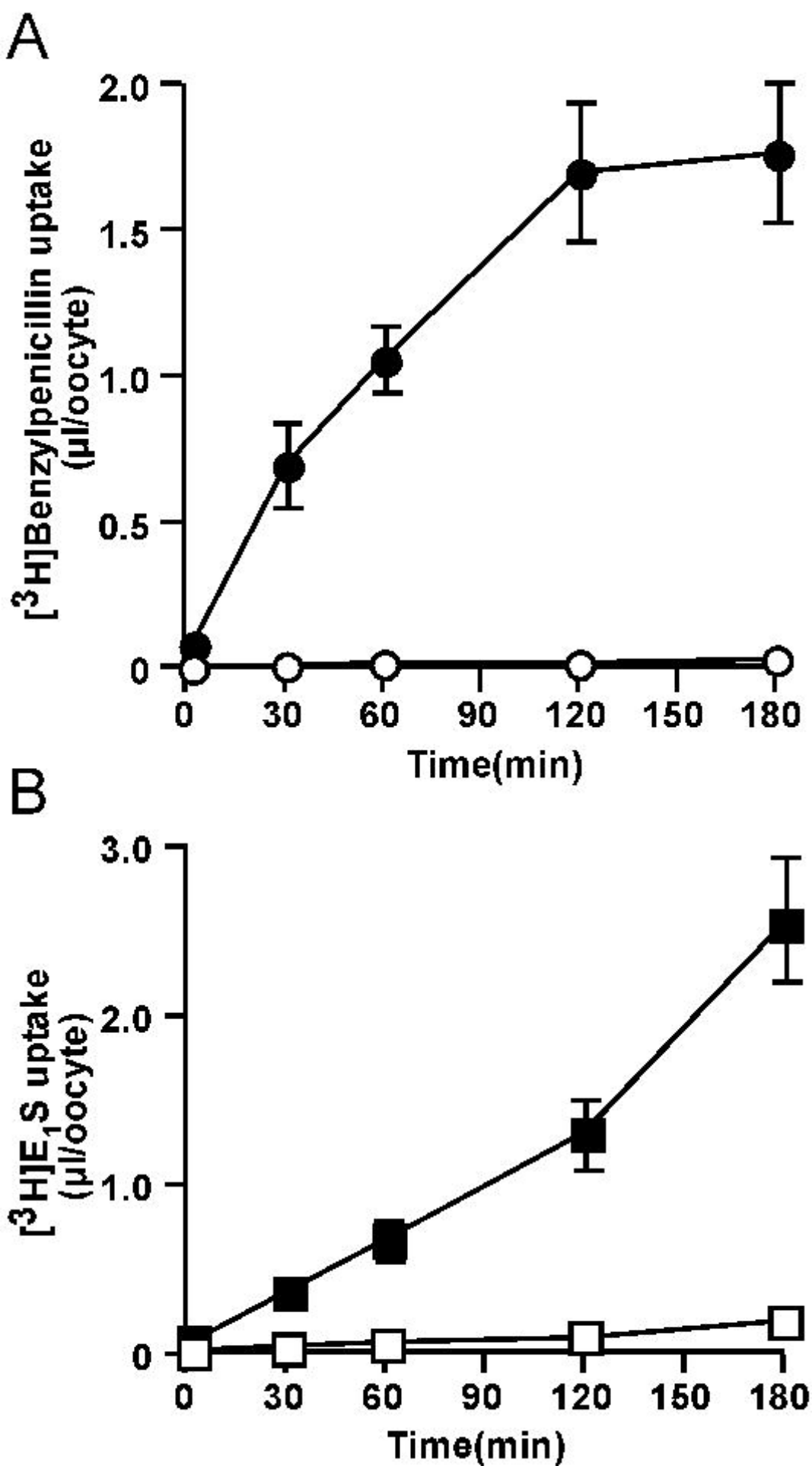
A
2.0
1.5
1.0
0.5
0
[3H]Benzylpenicillin uptake (µl/oocyte)
0
30
60
90
120
150
180
Time(min)
B
3.0
2.0
1.0
0
[3H]E1S uptake (µl/oocyte)
0
30
60
90
120
150
180
Time(min)

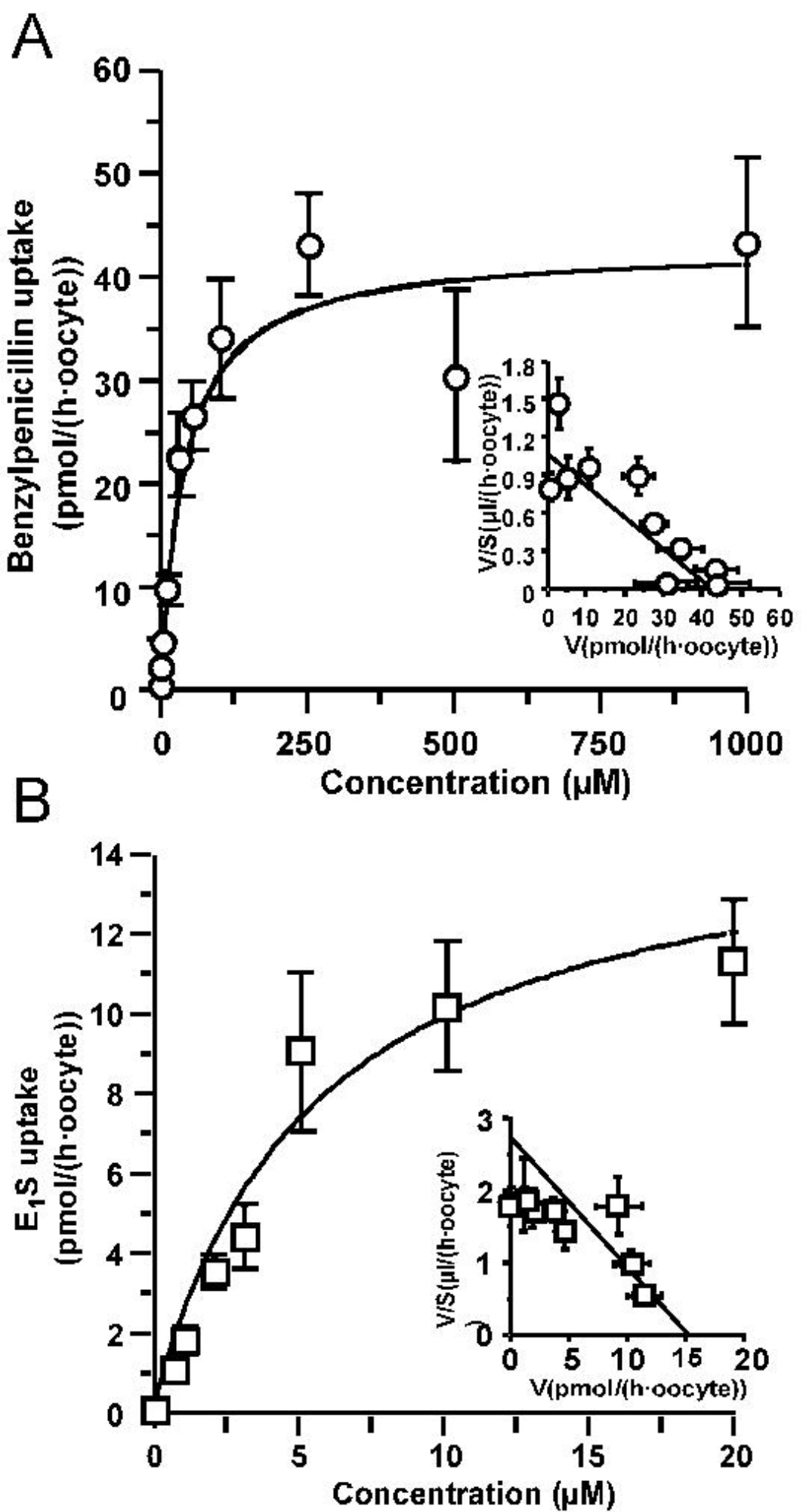
A
Benzylpenicillin uptake (pmol/(h·oocyte))
Concentration (μM)
V/S(μl/(h·oocyte))
V(pmol/(h·oocyte))
B
E1S uptake (pmol/(h·oocyte))
Concentration (μM)
V/S(μl/(h·oocyte)
V(pmol/(h·oocyte))

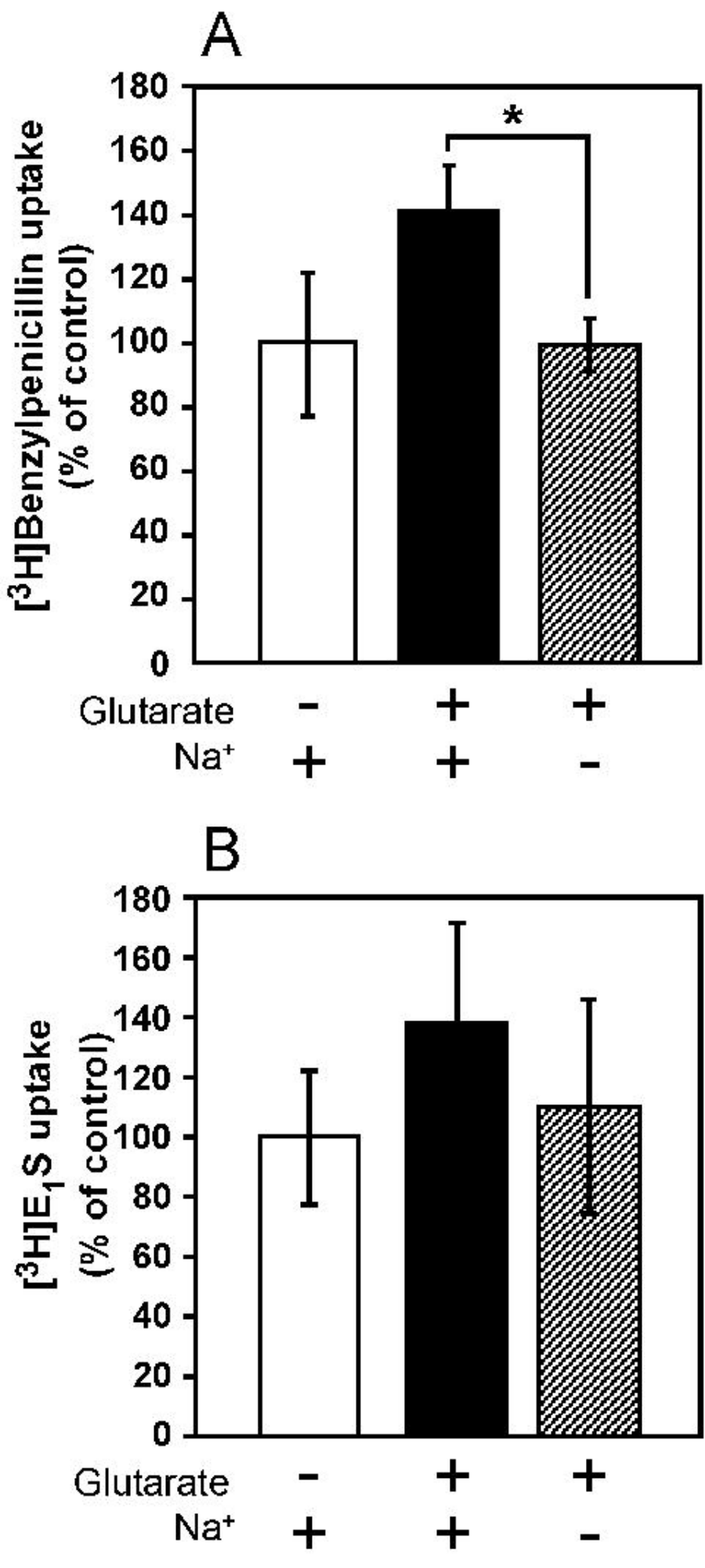
A
[3H]Benzylpenicillin uptake
(% of control)
180
160
140
120
100
80
60
40
20
0
*
Glutarate - + +
Na+ + + -
B
[3H]E1S uptake
(% of control)
180
160
140
120
100
80
60
40
20
0
Glutarate - + +
Na+ + + -

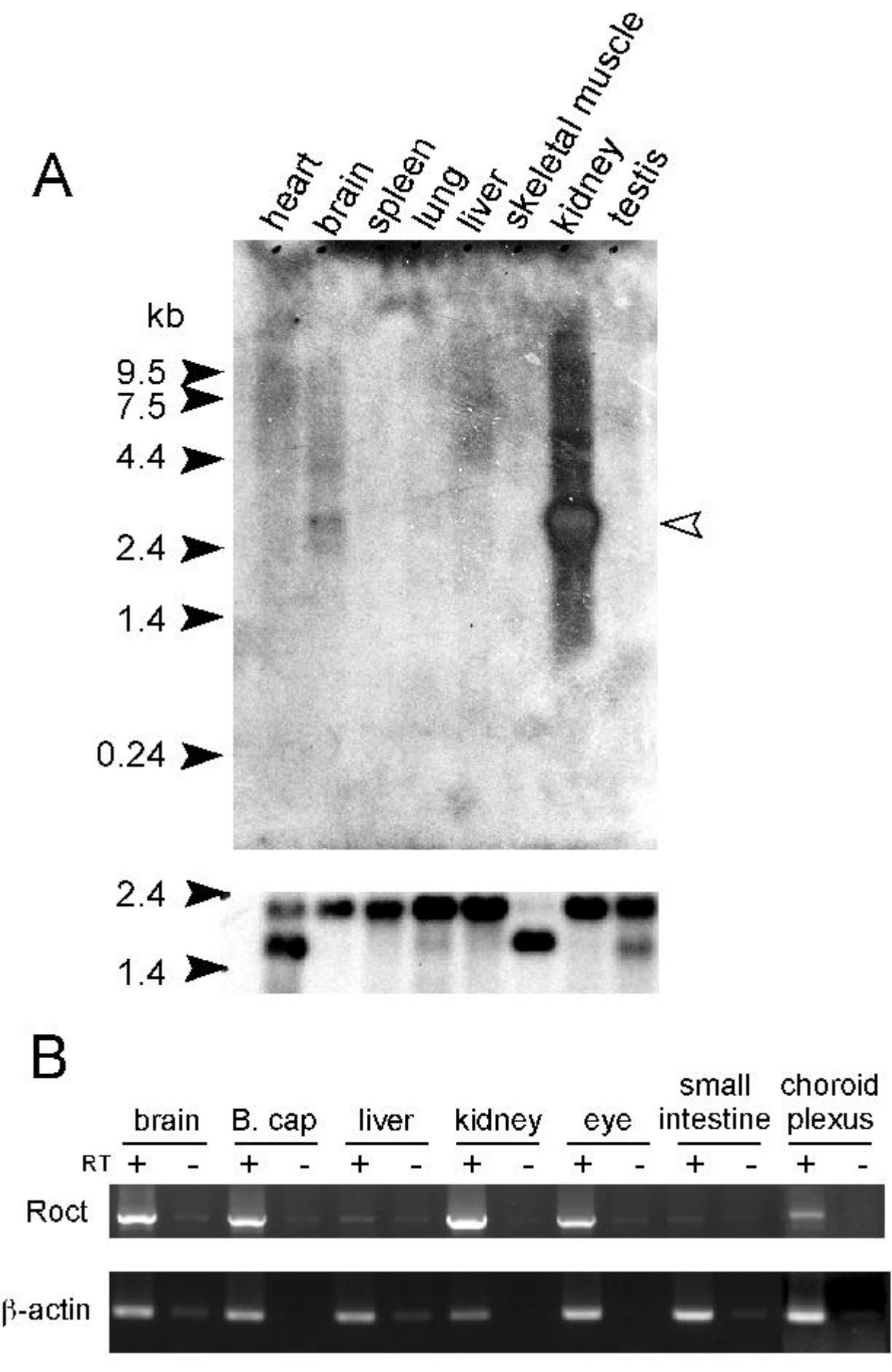
A
heart
brain
spleen
lung
liver
skeletal muscle
kidney
testis
kb
9.5
7.5
4.4
2.4
1.4
0.24
2.4
1.4
B
brain
B. cap
liver
kidney
eye
small intestine
choroid plexus
RT + - + - + - + - + - + - + -
Roct
β-actin

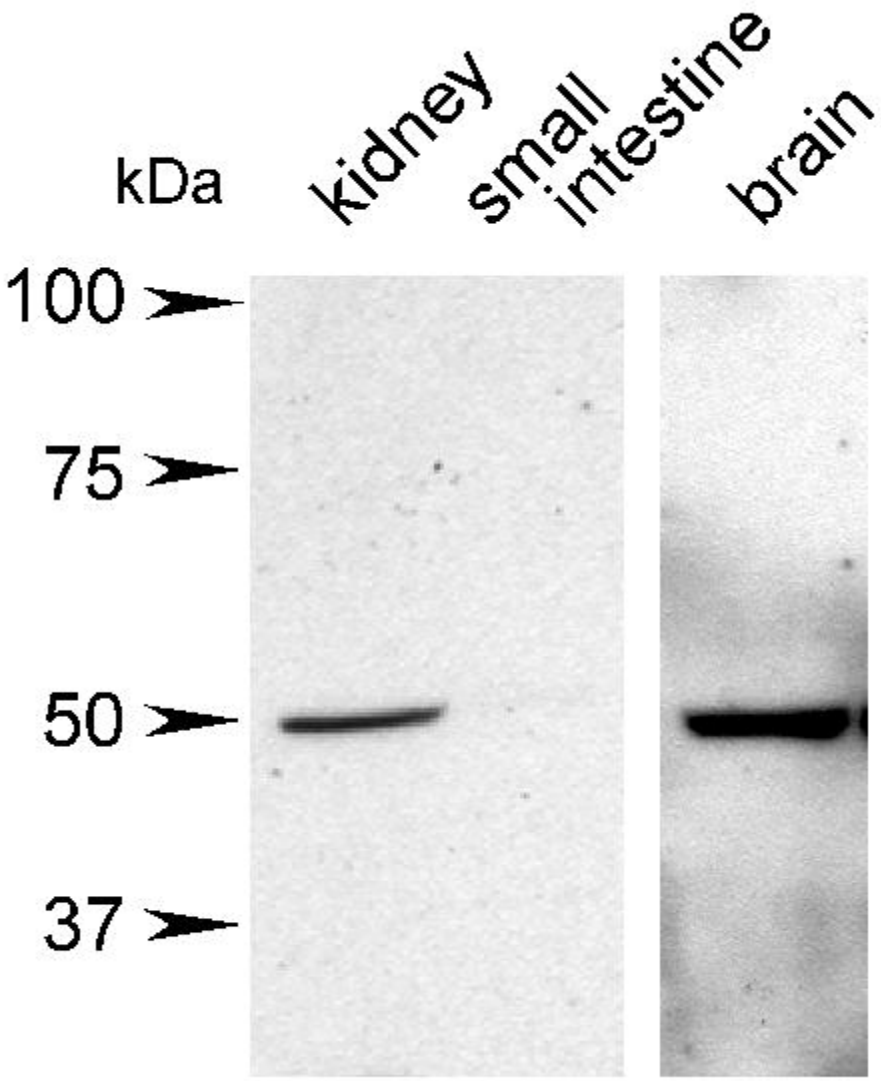
kDa
kidney
small intestine
brain
100
75
50
37

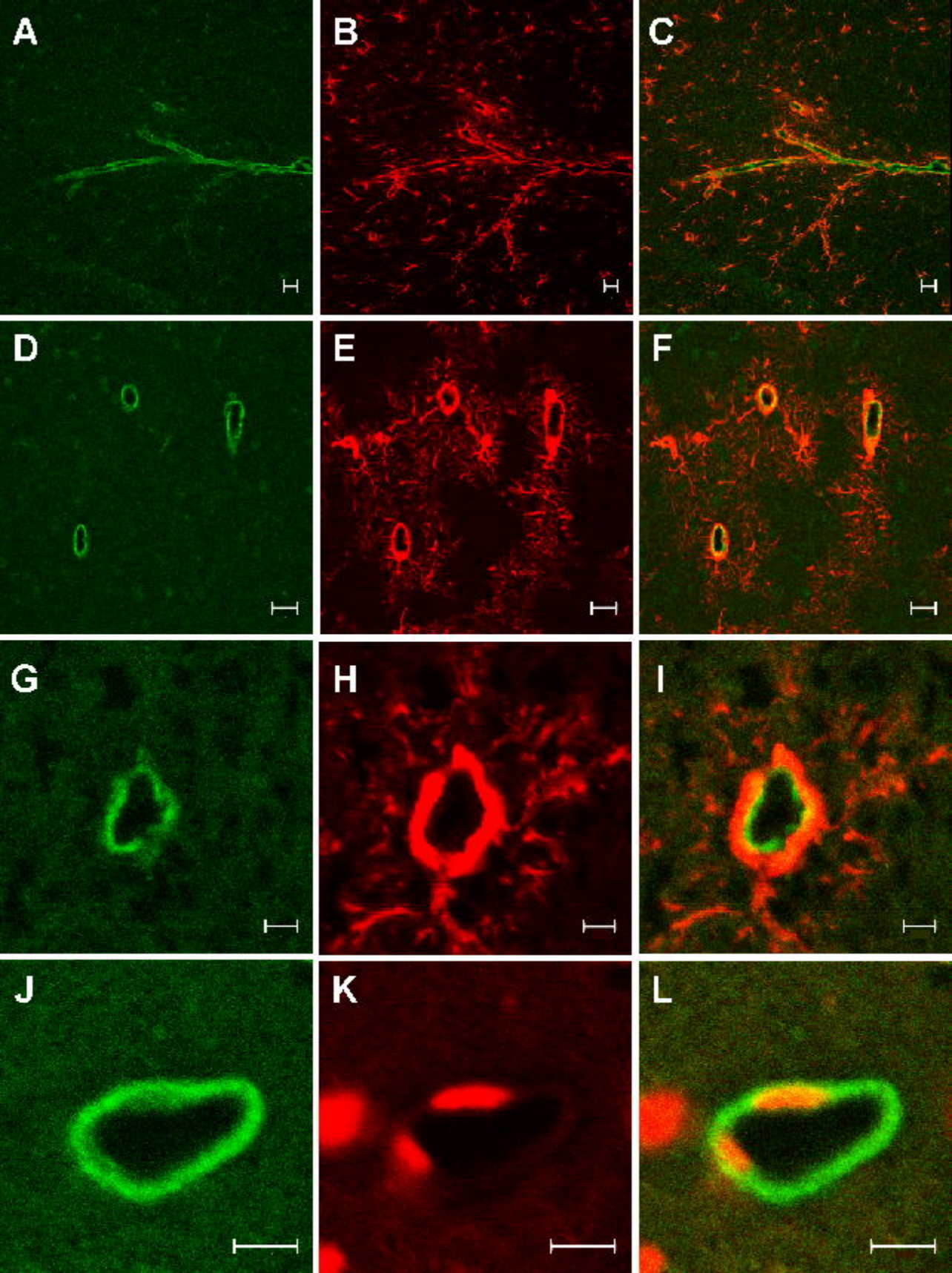
A
B
C
D
E
F
G
H
I
J
K
L